Available online at www.sciencedirect.com

SCIENCE DIRECT®

Inorganica Chimica Acta 345 (2003) 199–208

Inorganica Chimica Acta

www.elsevier.com/locate/ica

Neutral β-diketiminato nickel(II) monoalkyl complexes

Heather L. Wiencko, Elzbieta Kogut, Timothy H. Warren *

Department of Chemistry, Georgetown University, Washington, DC 20057, USA

Received 5 June 2002

Dedicated to Professor Richard R. Schrock

Abstract

Reaction of $NiCl_2$(2,4-lutidine)$_2$ (**1**) with Tl[Me_2NN] (**3**) in THF results in the transmetallation of the β-diketiminate ligand from which the tetrahedral {[Me_2NN]NiCl}$_2$ (**4**) was isolated in poor yield. After filtration of the TlCl formed in the reaction between **1** and **3** in THF, addition of Grignard reagents RMgBr results in the isolation of monoalkyl complexes [Me_2NN]Ni(R)(2,4-lutidine) (R = Me (**5**), Et (**6**), Pr (**7**)) in 40–70% yield. X-ray structures **5**–**7** of show these monoalkyls to be somewhat crowded, square planar species. NMR studies of the diamagnetic monoalkyl complexes show that lutidine dissociation/reassociation occurs on the NMR timescale at room temperature. In ethyl and propyl complexes **6** and **7**, an equilibrium between the four coordinate [Me_2NN]Ni(R)(2,4-lutidine) and a lutidine-free species [Me_2NN]Ni(R) (R = Et, Pr) is observed. Broad, high-field ^{1}H resonances consistent with the presence of β-H agostic alkyl groups are observed for the base-free species. The observation of two broad upfield ^{1}H NMR signals at δ -2.7 and -7.3 ppm for the base-free Ni–propyl complex suggests a mixture of primary and secondary β-agostic isomers that reversibly interconvert by β-H elimination/reinsertion. Ethylene slowly inserts into monoalkyls **5**–**7** demonstrate to give highly branched ethylene oligomers.

Keywords: β-Diketiminato nickel(II) complexes; Monoalkyl complexes; X-ray structures

1. Introduction

Later transition metal complexes attract attention as olefin polymerization catalysts due to their lower electrophilicity and resulting greater heteroatom tolerance as compared to early metal systems [1]. This significantly decreases the susceptibility of the late-metal catalysts to poisoning by polar monomers or polar impurities in the monomer feed [1,2]. An early example is the Shell Higher Olefin Process (SHOP) [3–5] developed by Keim et al. that employs monoanionic O$^\frown$P ligands in [$Ph_2PC(R)=C(R)O$]Ni(Ph)L (L = phosphine) complexes that catalyze the formation of linear α-olefins (C_6–C_{20}) from ethylene in 1,4-butanediol [6]. Only under forcing conditions [7] or in the presence of a phosphine scavenger [8], however, did these complexes polymerize ethylene to high molecular weight. Later work by Ostoja-Starzewski et al. and Klabunde et al. demonstrated that replacing the phosphine by more weakly coordinating neutral ligands in SHOP-like systems lead to similarly heteroatom tolerant catalysts capable of producing linear, high molecular weight polyethylene [9–14].

Brookhart's preparation and study of discrete Ni and Pd monoalkyl cations supported by α-diimine ligands highlighted key features important in late-metal ethylene polymerization catalysts [15–26]. While electrophilic, cationic metal centers that possess an accessible coordination site for an incoming olefin facilitate rapid olefin insertion, the use of bulky *N*-aryl groups slows associative chain transfer resulting in high molecular weight polymers [1]. Both the molecular weight and the degree of branching in the resulting polyethylenes can be controlled by choice of α-diimine substituents [15,17,21]. Furthermore, detailed NMR studies have identified the solution structures and dynamics of catalytically important species in the olefin polymerization catalytic cycle [19,20,22,24–26].

---

* Corresponding author. Tel.: +1-202-687 6362; fax: +1-202-687 6209.

E-mail address: thw@georgetown.edu (T.H. Warren).

0020-1693/02/$ - see front matter © 2002 Published by Elsevier Science B.V.
PII: S0020-1693(02)01310-5

Benefiting from these insights are new families of heteroatom tolerant, single-component neutral Ni(II) complexes possessing bulky O⌒N and N⌒N mononanionic ligands that are capable of polymerizing ethylene to high molecular weights [27,28]. Grubbs' family of neutral nickel complexes based on O⌒N salicylaldiminato ligands produces highly linear ethylene at rates that rival the highly active metallocenes [2,28,29]. Related O⌒N complexes based on anilinotroponates also show high activity but produce branched polyethylene whose branching numbers may be controlled by polymerization temperature and pressure [30]. Kläui et al. have developed a new family of O⌒N ligands that copolymerize ethylene and carbon monoxide at high rates and are also stable in the presence of excess CO [31]. Furthermore, he has shown that neutral N⌒N complexes based on bidentate, sterically hindered η^2-tris(pyrazolyl)borate [32] and semicorrine-type [31] monoanionic ligands are also competent ethylene and CO copolymerization catalysts.

While β-diketiminates ($[NN]^-$) have been investigated as ancillary ligands in cationic, early transition metal olefin polymerization catalysts [33–38], we sought the synthesis of well defined neutral monoalkyl complexes [NN]Ni(R)(L) that could be stabilized by an additional neutral base L (Fig. 1). Our initial efforts focused on the use of the mononanionic β-diketiminate ligand $[Me_2NN]^-$ derived from 2,4-bis(2,6-dimethylphenyllimido)pentane ($H[Me_2NN]$) [39,40]. Herein we describe the synthesis and X-ray structures of monoalkyl complexes $[Me_2NN]Ni(R)(L)$ along with NMR studies outlining their solution dynamics and alkene insertion behavior.

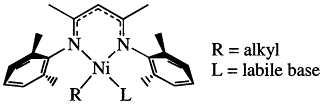

Fig. 1. Target β-diketiminato complexes.

2. Results

2.1. Synthesis and X-ray structures of β-diketiminato Ni(II) complexes

Aiming to prepare a β-diketiminate complex with a halide handle for alkylation, we explored the use of known $NiCl_2(2,4\text{-lutidine})_2$ (**1**) with several derivatives of $[Me_2NN]^-$. Reactions between **1** and the β-diketimine $H[Me_2NN]$ (**2**) as well as related β-diketiminato lithium and potassium salts in a variety of organic solvents did not lead to the isolation of any new Ni(II) complexes. Surprisingly, we did not observe the precipitation of insoluble LiCl or KCl, expected transmetallation products of reactions between **1** and $M[Me_2NN]$ (M = Li, K). Furthermore, the reaction with the potassium salt resulted in the formation of a nickel mirror, indicating reduction of the metal center. We then explored the use of a less reducing thallium derivative $Tl[Me_2NN]$ (**3**) [41] to encourage chloride removal from **1**.

While the reaction of **3** with **1** in THF results in the ready precipitation of TlCl, only in one solitary case were we able to unambiguously identify a reaction product. A few black crystals of dimeric $\{[Me_2NN]NiCl\}_2$ (**4**) were once isolated in very low yield (less than 5%) from THF after filtration of TlCl and we obtained its crystal structure (Scheme 1; Fig. 2). The β-diketiminate ligand symmetrically chelates the nickel center with bond distances of 1.913(3) and 1.915(3) Å (Table 1). The Ni–N bond distances in **4** are slightly shorter than those reported for the related tetrahedral bis(β-diketiminato) complexes $Ni(\eta^2\text{-}PhNC(Me)CHC(Me)NPh)_2$ (1.95(1)–1.97(1) Å) [42] and $Ni(\eta^2\text{-}ArNC(H)CPhC(H)NAr)_2$ (Ar = $p\text{-}ClC_6H_5$) (1.943(2) and 1.947(2) Å) [43] perhaps due to greater steric crowding in the homoleptic Ni(II) complexes. The N1–Ni–N2 angle of 94.69(11)° in **4** is in the range of 93.1(5)–95.0(5) observed for the bis(β-diketiminato) complexes. The lengthened ketiminate N–C bond distances of 1.330(4) and 1.338(4) Å in **4** are consistent with delocalization throughout the β-diketiminate fragment when compared to the shorter ketimine N=C distances of 1.280(8) and 1.269(8) Å found in the β-diketimine complex $[\eta^2\text{-}ArN{=}C(Me)CH_2C(Me){=}NAr]NiBr_2$ (Ar = 2,6-$^iPr_2C_6H_3$) [43]. The tetrahedral nickel centers in **5** are separated by 3.2966(8) Å and are essentially symmetrically bridged by two chlorides as shown by the similar Ni–Cl distances of 2.2997(9) and 2.3127(9) Å that form a Cl–Ni–Cl′ angle of 88.76(3)°.

While our inability to reproducibly prepare **4** precluded its use as a synthetic intermediate, filtration of the TlCl formed during the reaction of **1** and **3** followed by addition of Grignard reagents RMgCl provides the monoalkyl complexes $[Me_2NN]NiR(2,4\text{-lutidine})$ (R =

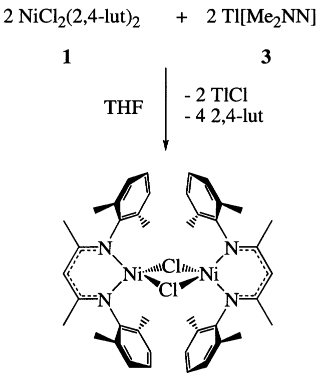

4

Scheme 1.

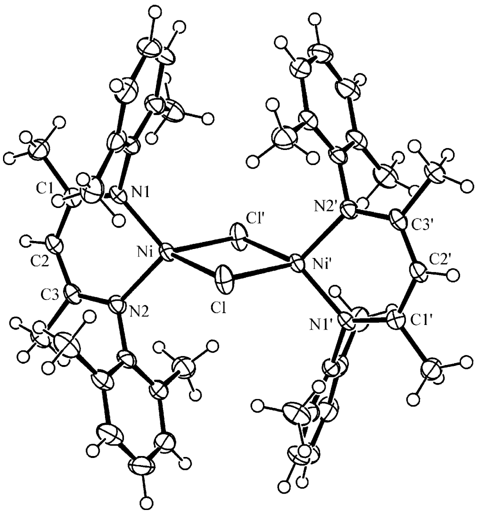

Fig. 2. ORTEP diagram of $\{[Me_2NN]NiCl\}_2$ (**4**).

Table 1
Bond distances (Å) and angles (°) in **4**

Bond distances	
Ni–N1	1.913(3)
Ni–N2	1.915(3)
Ni–Cl	2.3127(9)
Ni–Cl′	2.2997(9)
Bond angles	
N1–Ni–N2	94.69(11)
Cl–Ni–Cl′	88.76(3)
N1–Ni–Cl	110.50(8)
N1–Ni–Cl′	132.08(8)
N2–Ni–Cl	120.61(8)
N2–Ni–Cl′	112.97(9)

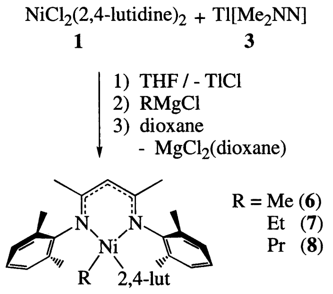

Scheme 2.

Me (**5**), Et (**6**), Pr (**7**)) as red crystals from ether in 40–70% yield (Scheme 2).

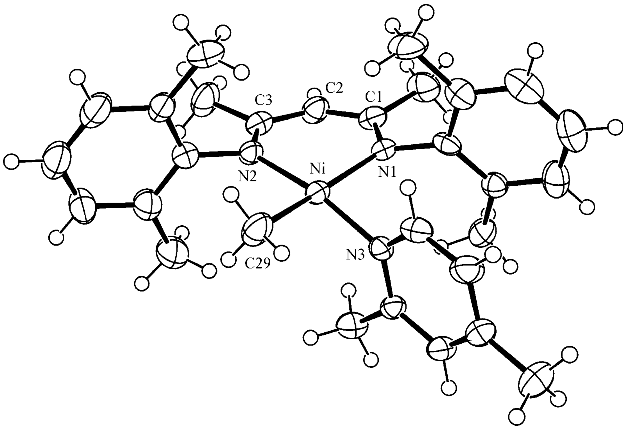

Fig. 3. ORTEP diagram of $[Me_2NN]Ni(Me)(2,4\text{-lutidine})$ (**5**).

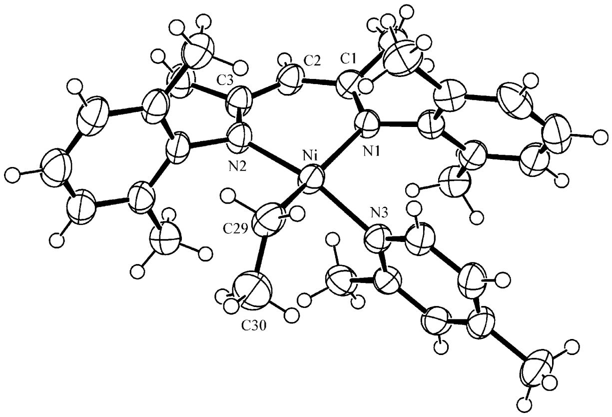

Fig. 4. ORTEP diagram of $[Me_2NN]Ni(Et)(2,4\text{-lutidine})$ (**6**).

In contrast to **4**, the X-ray structures of **5**–**7** (Figs. 3–5) reveal a square planar geometry about the nickel center as observed in other neutral four-coordinate Ni(II)-alkyl complexes [29,30,44–47]. Nearly identical metrical parameters are observed in each complex **5**–**7** (Table 2). Similar to tetrahedral **4**, the $[Me_2NN]^-$ ligand forms a 'bite' angle of 93.87(15)° in **5**. The longer Ni–N distance for the β-diketiminate donor opposing the Ni–alkyl group (Ni–N1 1.970(3) Å) compared to that opposite the 2,4-lutidine ligand (Ni–N2 1.906(4) Å) may be a result of a stronger *trans* influence for the alkyl ligand. Alternatively, this may be a reflection of the greater steric demands of the 2,4-lutidine ligand (Ni–N3 1.914(4) Å) perhaps amplified by the somewhat tight coordination pocket (C29–Ni–N3 84.55(17)°) flanked by the β-diketiminate *N*-aryl rings. The Ni–C_α distances

Table 2
Bond distances (Å) and angles (°) in **5**–**7**

	5	**6**	**7**
Bond distances			
Ni–N1	1.970(3)	1.987(3)	1.9716(17)
Ni–N2	1.906(4)	1.915(3)	1.9190(17
Ni–N3	1.914(4)	1.916(3)	1.9179(16)
Ni–C29	1.937(4)	1.965(4)	1.997(3)
C29–C30		1.497(7)	1.518(6)
Bond angles			
N1–Ni–N2	93.87(15)	93.16(12)	93.57(7)
C29–Ni–N3	84.55(17)	86.74(14)	81.01(10)
N3–Ni–N2	169.83(15)	163.19(14)	167.76(8)
N1–Ni–C29	168.4(2)	157.95(17)	172.60(10)
Ni–C29–C30		119.9(3)	107.1(3)

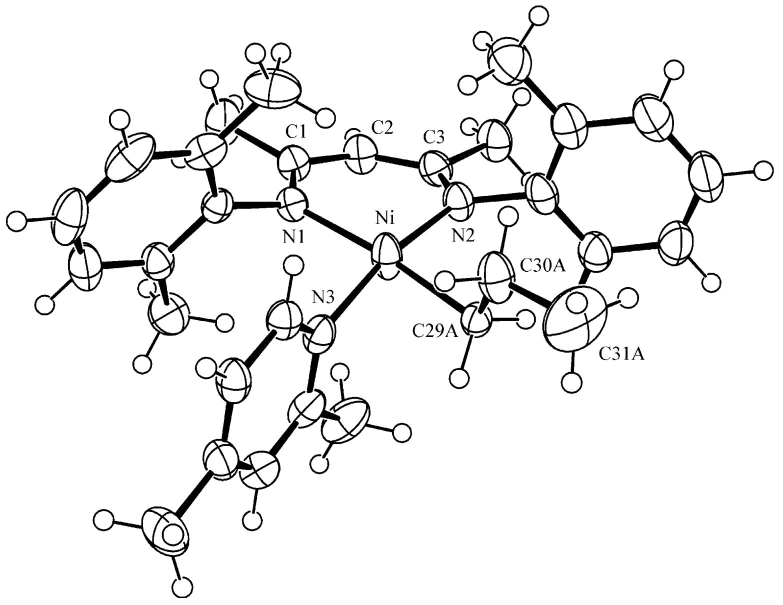

Fig. 5. ORTEP diagram of [Me$_2$NN]Ni(Pr)(2,4-lutidine) (**7**). The propyl group (C29–C31) is disordered over two sets of positions; only the major (60%) occupancy is shown.

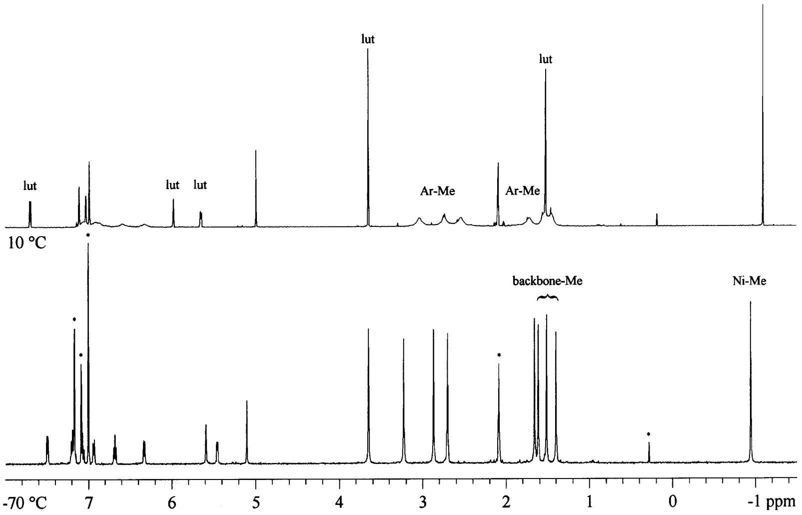

Fig. 6. Variable temperature ^{1}H NMR spectra of **5** (500 MHz, toluene-d$_8$).

increase with the length of the alkyl group (1.937(4), 1.965(4), 1.997(3) Å for **5**, **6**, **7**, respectively) and the Ni–C29–C30 angles in the ethyl and propyl complexes **7** and **8** of 119.9(3) and 107.1(3)° do not indicate the presence of β-agostic interactions in these four-coordinate species.

2.2. Solution behavior probed by NMR spectroscopy

^{1}H and ^{13}C NMR spectra of **5**–**7** taken at low temperature (approximately −40 °C) are consistent with their structures in the solid state. Six diastereotopic β-diketiminate methyl signals are observed as a consequence of the *o*-Me group of the lutidine being out the square plane of the complex. Low temperature ^{1}H NMR spectra in toluene-d$_8$ reveal upfield signals for the Ni–alkyl α-H atoms. The Ni–CH_3 resonance in **5** appears as a singlet δ −1.64 ppm while the Ni–CH_2 resonances for **6** and **7** consist of two diastereotopic multiplets each at δ 0.13 and 0.06 ppm and δ −0.04 and −0.50 ppm, respectively, consistent with the C_1 symmetry of **5**–**7**.

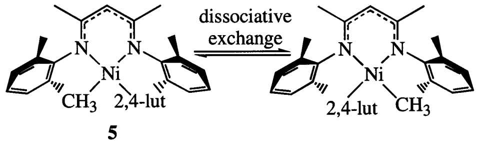

5

Scheme 3.

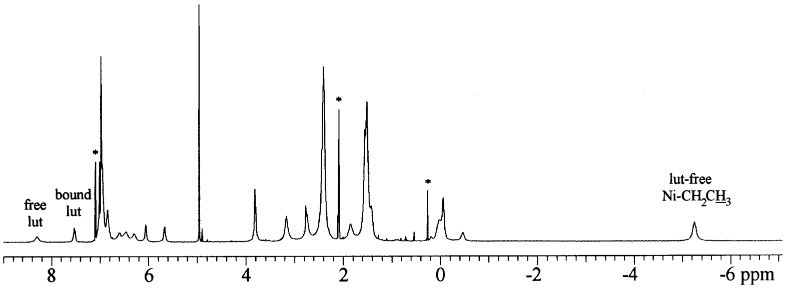

Fig. 7. Room temperature ^1H NMR spectrum of **6** (300 MHz, toluene-d_8).

Variable temperature ^1H NMR spectra of these monoalkyls demonstrate that 2,4-lutidine is labile in these complexes. Gradually warming a toluene-d_8 solution of **5** results in the broadening of all β-diketiminate signals except for the backbone C–H group (Fig. 6). This behavior is consistent with the reversible dissociation/reassociation of 2,4-lutidine (Scheme 3). Identifying the exact coalescence temperature for the backbone Me groups (16(2) °C at 300 MHz) allowed us to establish an activation barrier $\Delta G^{\neq} = 12.1(3)$ kcal mol^{-1} at this temperature. An associative mechanism for exchange was ruled out as there is no change in the coalescence temperature in the presence of added 2,4-lutidine.

The variable temperature behavior of the β-H containing monoalkyls **6** and **7** is markedly different than that observed for **5**. At room temperature in toluene-d_8, ethyl complex **6** exhibits new aromatic resonances corresponding to free lutidine as well as a broad resonance at δ −5.3 ppm of area 3 relative to the released lutidine (Fig. 7). These new resonances increase in intensity as the temperature is raised to 40 °C. These observations are consistent with the reversible loss of lutidine to produce an observable concentration of the lutidine-free [Me_2NN]NiEt (**8**). Due to the significantly upfield-shifted Ni–CH_2CH_3 resonance observed, we suggest that the ethyl group in **8** assumes a β-agostic structure [19,20,24,26,48] in which a β-C–H bond interacts with the coordination site left vacant by the 2,4-lutidine (Scheme 4). The observation of a single β-H resonance of area 3 indicates that rotation about the ethyl C–C bond is rapid at these temperatures. The temperature dependence of the equilibrium constant for lutidine dissociation measured by ^1H NMR allows the determination of $\Delta H = 8.3$ (3) kcal mol^{-1} and $\Delta S = 20$ (3) cal mol^{-1} K for this process.

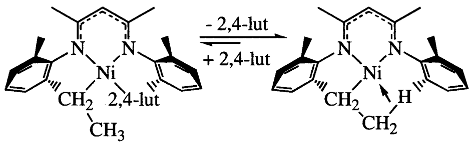

6 **8**

Scheme 4.

While unbound lutidine also appears in the room temperature ^1H NMR spectrum of Ni–propyl complex **7** in toluene-d_8, *two* broad upfield signals at δ −2.7 and −7.3 ppm are observed (Fig. 8) suggesting the presence of two different β-H agostic Ni–propyl species at room temperature. While these upfield resonances have not been unequivocally assigned due to their broad nature, both a primary (linear) and a secondary (branched) β-H agostic propyl group would be expected if β-H elimination followed by reinsertion readily occurs upon disassociation of lutidine [24]. This process is reversible; cooling regenerates the four-coordinate primary alkyl [Me_2NN]Ni(Pr)(2,4-lutidine) (Scheme 5).

2.3. Ethylene reactivity

Addition of approximately 3 equiv. of ethylene to methyl and ethyl complexes **5** and **6** in benzene-d_6 at 1 atm and room temperature results in the observation of broad upfield ^1H NMR signals at δ −2.7 and −7.3 ppm after 2–3 min. These signals are similar to those observed for the propyl complex **7**, suggesting the presence of both linear and branched Ni–alkyl chains formed by the insertion of ethylene into the original Ni–C bonds present in **5** and **6**. While both the ethylene ^1H NMR signal at δ 5.24 ppm and the upfield ^1H resonance of base-free **8** at δ −5.3 ppm were completely consumed after approximately 10 min, the Ni–Me resonance of **5** at δ −1.64 ppm could still be observed after complete consumption of ethylene. This suggests that the extent of lutidine dissociation may be an important factor in determining the rate of ethylene insertion. Exposure of **6** to 100 psi ethylene in toluene at room temperature for 10 min followed cleavage of all Ni–alkyl chains by an acidic workup results in a distribution of C_8–C_{18} oligomers in which each C_{2n+2} fraction consists of several resolved isomers. The presence of highly branched oligomers is consistent with the above NMR studies and indicate that isomerization via β-H elimination/reinsertion is fast compared to insertion [24]. Initiation with Ni–propyl complex **7** under identical conditions leads to the exclusive production of C_{2n+1} oligomers, showing that each Ni center produces only one alkyl chain.

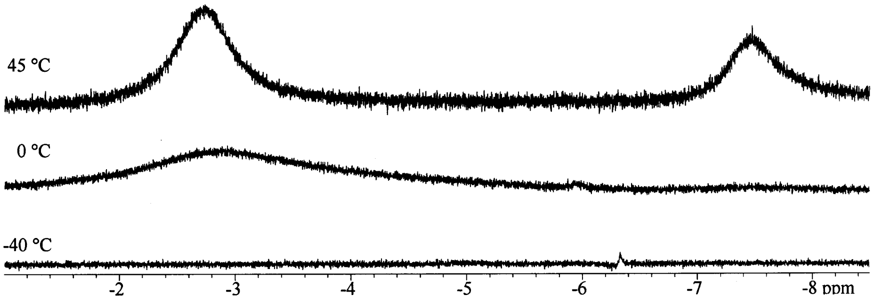

Fig. 8. Variable temperature ^1H NMR spectra of upfield region of **7** (300 MHz, toluene-d_8).

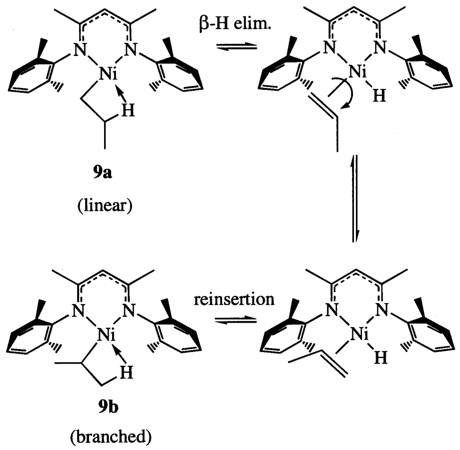

Scheme 5.

3. Discussion and conclusion

We were originally attracted to 2,4-lutidine as a potentially labile base in our targeted four-coordinate monoalkyl complexes by Schrock's finding that 2,4-lutidine can serve as a stabilizing, yet labile base in the molybdenum imido alkylidene complex Mo(CHC-Me_2Ph)(NAd)[$OCH(CF_3)_2]_2$(2,4-lutidine) (Ad = 1-adamantyl) that catalyzes the polymerization of (*o*-(trimethylsilyl)phenyl)acetylene [49]. The use of 2,4-lutidine results in the crystalline, easily isolable four-coordinate [Me_2NN]Ni(R)(2,4-lutidine) complexes **5**–**7** that readily dissociate the lutidine base in solution. In the case of the β-H containing ethyl and propyl complexes **6** and **7**, ^1H NMR data indicate a reversible, temperature dependent equilibrium between lutidine-bound and lutidine-free species. β-H elimination/reinsertion is a facile, reversible process that is rapid relative to ethylene insertion and results in the formation of highly branched short chain oligomers.

While β-agostic interactions in cationic late-metal systems are well established and play an important role in the branching of metal–alkyl chains via β-H elimination/reinsertion, these interactions are far less commonly observed in neutral systems. β-H agostic interactions in neutral, early transition metal complexes have been suggested on the basis of spectroscopic data for Sc [50], Ti [51], and Ta [52] as well as demonstrated in the X-ray structures of $TiCl_3$(dmpe)Et [53,54] and [P_2N_2]Ta(CH_2CH_2)Et ([P_2N_2]=PhP($CH_2SiMe_2NSiMe_2CH_2)_2$PPh) [55]. The more electron-rich, β-diketiminato Ni–ethyl and Ni–propyl complexes discussed herein may favor β-agostic interactions due to a more compact coordination wedge as compared to neutral O⌒P and O⌒N systems due to the presence of two β-diketiminato *N*-aryl substituents, favoring loss of a neutral base. Chemical removal of 2,4-lutidine from **6** and **7** would allow a more detailed investigation into these neutral, base-free β-agostic alkyls [Me_2NN]NiR (R = Et (**8**), Pr) and will be reported elsewhere shortly.

4. Experimental

4.1. General experimental details

All experiments were carried out in a dry nitrogen atmosphere using an MBraun glovebox and/or standard Schlenk techniques. 4A molecular sieves were activated in vacuo at 180 °C for 24 h. Dry $C_6H_5CH_3$ was purchased from Aldrich and was stored over activated 4A molecular sieves. Benzene, Et_2O, tetrahydrofuran (THF) and C_5H_{12} were distilled before use from sodium/benzophenone and CH_2Cl_2 was distilled from CaH_2. All deuterated solvents were sparged with nitrogen, dried over activated 4A molecular sieves and stored under nitrogen. ^1H and ^{13}C NMR spectra were recorded either on a Mercury Varian 300 MHz spectrometer (300 and 75.4 MHz, respectively) or a Varian Unity 500 MHz spectrometer (500 and 125.6 MHz) at 25 °C unless otherwise noted. The NMR spectra were indirectly referenced to TMS using residual solvent signals as internal standards. 2,4-Lutidine was obtained from Aldrich and stored over 4A molecular sieves prior to use. Anhydrous $NiCl_2$ was obtained from Strem and ethylene from MG industries; all were used as received. All Grignard reagents were obtained from Aldrich and titrated directly before use. 2,4-Bis(2,6-dimethylphenylimido)pentane, (H[Me_2NN]) (**3**) [39,40] and Tl[Me_2NN]

(**4**) [41] were synthesized according to literature procedures.

4.2. Preparation of $NiCl_2(2,4\text{-}lut)_2$ (**1**)

Adapted from a literature procedure [56]: anhydrous $NiCl_2$ (1.87 g, 14.4 mmol) was suspended in 11 ml 2,4-lutidine (neat) and heated to 80 °C. The suspension turned from yellow to bright purple in approximately 7 min. The resulting solution was filtered hot through Celite. Purple crystals of $NiCl_2(2,4\text{-lut})_2$ began to form immediately. The crystals that formed were isolated and washed with pentane to afford a total yield of 3.13 g (91.8%) of purple crystals.

4.3. Isolation of $\{[Me_2NN]NiCl\}_2$ (**4**)

Tl[Me_2NN] (1.00 g, 1.96 mmol) in 2 ml THF was added to a stirring suspension of **1** (0.465 g, 1.96 mmol) in approximately 5 ml THF. A white precipitate formed quickly. After stirring for 1 h, the solution was filtered through Celite to remove TlCl, concentrated, and left to stand for 2 days at −30 °C. A few black crystals formed and one was characterized by X-ray.

4.4. Preparation of [Me_2NN]NiMe(2,4-lut) (**6**)

[Me_2NN]Tl (2.51 g, 4.93 mmol) was dissolved in 5 ml THF and added with stirring to a suspension of $NiCl_2(2,4\text{-lut})_2$ (1.69 g, 4.93 mmol) in 15 ml THF. Over 5 min, the solution turned deeper purple and became cloudy. The precipitate was then allowed to settle and the solution was filtrated through Celite. After chilling the filtrate to −35 °C, a solution of MeMgBr (1.44 ml, 4.93 mmol, 3.42 M in Et_2O) in 5 ml THF was added with stirring. The purple solution turned orange–red immediately, becoming deeper in color over 5 min. The volatiles were removed in vacuo and the remaining solids were dissolved in 20 ml ether. The Mg salts were precipitated by addition of dioxane (0.434 g, 4.93 mmol) with stirring. After the solids were allowed to settle, the solution was filtered through Celite and the filtrate was concentrated leading to partial crystallization. The solution was left to further crystallize at −35 °C overnight. Red–orange crystals were collected on a frit, washed with ether (5 ml), and dried by vacuum to afford 1.052 g (44% yield) of the product. ^{1}H NMR (THF-d_8, −40 °C): δ 7.68 (d, 1, lut), 6.95, 6.92, 6.91, 6.80, 6.79, 6.77, 6.75 (aromatic), 6.60 (t, 1, Ar), 6.37 (d, 1, Ar), 6.19 (d, 1, Ar–lut), 4.80 (s, 1, *H*-backbone), 3.78 (s, 3, lut–CH_3), 2.98 (s, 3, Ar–CH_3), 2.52 (s, 3, Ar–CH_3), 2.28 (s, 3, Ar–CH_3), 2.05, 1.72, 1.36, 1.32 (s, 3, CH_3; 1 Ar–Me, 1 lut–Me, 2 backbone Me), −1.64 (s, 3, Ni–CH_3); ^{13}C NMR (THF-d_8, −40 °C): δ 159.07, 158.93, 158.55, 152.49, 151.45, 151.02, 146.74, 133.46, 133.16, 132.20, 131.81, 128.14, 128.11, 127.92, 127.86, 124.93, 123.78, 123.49, 122.16, 97.12 (backbone C), 27.61, 25.38, 23.96, 20.49, 19.58, 18.12, 15.96, −4.10 (Ni–CH_3); *Anal.* Calc. for $C_{29}H_{37}N_3$: C, 71.59; H, 7.68; N, 8.64. Found: C, 71.42; H, 7.65; N, 8.15%.

4.5. Preparation of [Me_2NN]NiEt(2,4-lut) (**7**)

Tl[Me_2NN] (3.00 g, 5.90 mmol) was dissolved in 5 ml THF and added to a stirring suspension of **1** (2.02 g 5.90 mmol) in 10 ml THF at room temperature (r.t.). The purple solution immediately turned deeper purple and became cloudy. Thallium chloride was removed by filtration through Celite. A chilled (−30 °C) solution of CH_3CH_2MgCl (2.58 ml, 5.90 mmol, 2.29 M in Et_2O) in 5 ml THF was added with stirring to the chilled (−30 °C) filtrate. The purple solution turned red quickly, deepening in color over 3 min. The THF was removed under vacuum and the remaining solids were extracted with 15 ml ether. Magnesium salts were precipitated by the addition of dioxane (0.52 g, 5.9 mmol) with stirring. The mixture was filtered through Celite, and the filtrate was concentrated to 7 ml under vacuum. Crystallization occurred as the solution was concentrated, and the solution was left to stand at −35 °C overnight. The crystals that formed were collected and dried under vacuum to afford a total yield of 2.024 g (69%) of red–orange crystals in two crops. ^{1}H NMR ($C_6H_5CH_3$-d_8, −40 °C): δ 7.47 (d, 1, lut), 7.13, 7.11, 7.09, 7.05, 7.04, 7.01, 6.99, 6.95 (aromatic), 6.65 (t, 1, lut), 6.31 (d, 1, lut), 5.87 (s, 1, lut), 5.59 (d, 1, lut), 5.03 (s, 1, *H*-backbone), 3.79 (s, 3, lut-CH_3), 3.25 (s, 3, Ar–CH_3), 2.81 (s, 3, Ar–CH_3), 2.54 (s, 3, Ar–CH_3), 1.61, 1.55, 1.49, 1.45 (s, 3, CH_3; 1 Ar–Me, 1 lut–Me, 2 backbone Me), 0.13 (q, 1, NiCH_2CH_3), 0.06 (q, 1, NiCH_2CH_3), −0.43 (t, 3, NiCH_2CH_3); ^{13}C NMR (THF-d_8, −40 °C): δ 159.66, 158.81, 158.77, 151.98, 151.41, 150.38, 146.73, 133.75, 133.50, 132.58, 131.71, 128.54, 128.26, 128.01, 127.91, 124.94, 123.95, 123.46, 121.79, 97.28 (backbone C), 27.42, 23.80, 20.73, 20.45, 19.76, 19.36, 17.83, 13.84 (Cβ), 8.84 (Cα); $J_{C\alpha\text{–}H} = 128.07$ Hz, $J_{C\beta\text{–}H} = 124.68$; *Anal.* Calc. for $C_{30}H_{39}N_3$: C, 72.01; H, 7.87; N, 8.40%. Found: C, 71.71; H, 7.92; N, 8.20.

4.6. Preparation of [Me_2NN]NiPr(2,4-lut) (**8**)

Tl[Me_2NN] (0.714 g, 1.40 mmol) was dissolved in 2 ml THF and added to a stirring suspension of **1** (0.481g 1.40 mmol) in 5 ml THF at r.t. The purple solution immediately turned deeper purple and became cloudy. After removal of the TlCl precipitate, a chilled (−30 °C) solution of $CH_3CH_2CH_2MgCl$ (0.70 ml, 1.4 mmol, 2.0 M in Et_2O) in 2 ml THF was added with stirring to the chilled (−30 °C) filtrate. The purple solution turned red quickly, deepening in color over 3 min. The THF was removed under vacuum and the remaining solids were dissolved in 10 ml ether. Magnesium salts were precipitated by the addition of dioxane (0.12 g, 1.4 mmol) with stirring. The mixture was filtered through Celite, and the filtrate was concentrated to 4 ml under vacuum. Crystallization occurred as the solution was being concentrated, and the solution was left to stand at −35 °C overnight. The crystals that formed were collected and dried under vacuum to afford 0.423 g (62%) of red crystals in one crop. ^{1}H NMR ($C_6H_5CH_3$-d_8, −50 °C): δ 7.47 (d, 1, lut), 7.13, 7.11, 7.09, 7.05, 7.04, 7.01, 6.99, 6.96 (aromatic), 6.65 (t, 1, lut), 6.30 (d, 1, lut), 5.84 (s, 1, lut), 5.57 (d, 1, lut), 5.02 (s, 1, *H*-backbone), 3.79 (s, 3, lut–CH_3), 3.28 (s, 3, Ar–CH_3), 2.82 (s, 3, Ar–CH_3), 2.53 (s, 3, Ar–CH_3), 1.62, 1.55, 1.47, 1.44 (s, 3, CH_3; 1 Ar–Me, 1 lut–Me, 2 backbone Me), 1.85 (m, 1, $\mathrm{NiCH_2}\mathit{CH_A}\mathrm{H_B}$), 0.91 (m, 1, $\mathrm{NiCH_2CH_A}\mathit{H_B}$), 0.56 (t, 3, $\mathrm{NiCH_2CH_2}\mathit{CH_3}$), −0.037 (m, 1, $\mathrm{Ni}\mathit{CH_A}\mathrm{H_B}$), −0.502 (m, 1, $\mathrm{NiCH_A}\mathit{H_B}$); ^{13}C NMR (THF-$d_8$): δ 159.29, 158.47, 158.41, 151.76, 151.13, 150.13, 146.49, 133.59, 133.24, 132.28, 131.38, 128.09, 127.81, 124.72, 123.74, 123.29, 121.66, 123.46, 97.22 (backbone C), 27.54, 24.04, 23.12, 20.98, 20.59, 20.02, 19.58, 17.94 (Cβ), 16.33 (Cγ), 16.08 (Cα); *Anal.* Calc. for $C_{31}H_{41}N_3Ni$: C, 72.39; H, 8.03; N, 8.17. Found: C, 72.54; H, 8.18; N, 7.82%.

4.7. Determination of ΔH and ΔS for $[Me_2NN]Ni(2,4\text{-}lut)Et$

A sample of $[Me_2NN]Ni(2,4\text{-}lut)Et$ (0.047 g, 0.094 mmol) was dissolved in 1 ml of $C_6H_5CH_3$-d_8 in a volumetric flask and transferred in to NMR tube. ^{1}H NMR spectra were acquired every 10 °C over the range of temperatures −30–60 °C. The integration of resonances corresponding to free (δ 8.38 ppm) and bound lutidine (δ 7.47 ppm) as well as β-agostic species (δ −5.26 ppm) against an internal standard (C_5H_{12}) allowed the calculation of the equilibrium constants at different temperatures using the following dependence:

$$K_{eq} = \{[\text{free lutidine}][\beta\text{-agostic}]/[\text{bound lutidine}]\} \times [\text{initial concentration}]$$

A van't Hoff plot of $\ln K$ versus $1/T$ allowed the calculation of ΔH (slope) and ΔS (intercept).

4.8. Addition of ethylene to **5**

Complex **5** (0.030 g, 0.060 mmol) was placed into an NMR tube and dissolved in C_6D_6. One equiv. of ethylene at 1 atm was added by syringe and ^{1}H spectra were taken. After 2 min, new β-agostic signals at δ −2.7 and −7.3 ppm appeared. Although the signal at δ 5.24 ppm (C_2H_4) disappeared after 30 min, the signal at δ −1.64 ppm (Ni–CH_3) remained throughout the experiment, suggesting propagation occurs more readily than initiation.

4.9. Addition of ethylene to **6**

Complex **6** (0.030 g, 0.059 mmol) was placed into an NMR tube and dissolved in C_6D_6. One equiv. of ethylene at 1 atm was added by syringe and ^{1}H spectra were taken. After 2 min, new β-agostic signals at δ −2.7 and −7.3 ppm appeared. The signals at δ 5.24 ppm (C_2H_4) and −5.27 ppm (Ni–CH_2CH_3) had disappeared after 30 min, suggesting propagation and initiation occur at comparable rates.

4.10. Structure determinations and crystal data for **4**–**7**

Single crystals of each compound were mounted under mineral oil on glass fibers and immediately placed in a cold nitrogen stream at −100(2) °C on a Bruker SMART CCD system. Full spheres of data were collected (0.3° ω-scans; $2\theta_{max} = 56°$; monochromatic Mo Kα radiation, $\lambda = 0.7107$ Å) and integrated with the Bruker SAINT program. Structure solutions were performed using the SHELXTL/PC suite and XSEED [57–59]. Intensities were corrected for Lp effects and an empirical absorption correction was applied using Blessing's method as incorporated into the program SADABS [60]. Non-hydrogen atoms were refined with aniostropic thermal parameters and hydrogen atoms were included in idealized positions. Positional disorder was observed in the propyl group of **7** and was modeled using a 60/40 ratio of two different orientations (C29A–C30A–C31A/C29B–C30B–C31B).

4.10.1. Crystal/refinement details for **4**

$C_{21}H_{25}ClN_2Ni$, $M = 399.59$, black crystal $0.32 \times 0.20 \times 0.12$ mm, monoclinic, space group $P2(1)/c$, $a = 12.8726(15)$, $b = 8.9541(10)$, $c = 17.384(2)$ Å, $\beta = 103.535(2)°$, $V = 1948.1(4)$ Å^3, $Z = 4$, $\mu = 1.138$ mm^{-1}, empirical absorption correction ($0.75 \le T \le 1.00$), 21 627 reflections collected at −100 °C, 4759 independent reflections ($R_{int} = 0.0829$), 3352 reflections observed [$I > 2\sigma(I)$], 233 refined parameters, $R_1 = 0.0600$, $wR_2 = 0.1380$ (observed reflections), $R_1 = 0.0968$, $wR_2 = 0.1505$ (all data), max. residual electron density 0.756 and −1.236 e Å^{-3}.

4.10.2. Crystal/refinement details for **5**

$C_{29}H_{37}CN_3Ni$, $M = 486.33$, orange plate $0.20 \times 0.18 \times 0.08$ mm, monoclinic, space group $P2(1)/n$, $a = 7.759(4)$, $b = 21.837(10)$, $c = 15.861(7)$ Å, $\beta = 104.137(14)°$, $V = 2606(2)$ Å^3, $Z = 4$, $\mu = 0.765$ mm^{-1}, empirical absorption correction ($0.79 \le T \le 1.00$), 25 917 reflections collected at −100 °C, 5132 independent reflections ($R_{int} = 0.1605$), 2228 reflections observed [$I > 2\sigma(I)$], 308 refined parameters, $R_1 = 0.0536$, $wR_2 = 0.1104$ (observed reflections), $R_1 = 0.1615$, $wR_2 = 0.1284$ (all data), max. residual electron density 0.487 and −0.441 e Å^{-3}.

4.10.3. Crystal/refinement details for ***6***

$C_{30}H_{39}N_3Ni$, $M = 500.35$, red chunk $0.38 \times 0.44 \times 0.45$ mm, orthorhombic, space group $P2(1)2(1)2(1)$, $a = 9.8201(15)$, $b = 10.8194(10)$, $c = 25.541(3)$ Å, $V = 2713.6(7)$ Å^3, $Z = 4$, $\mu = 0.737$ mm^{-1}, empirical absorption correction ($0.76 \leq T \leq 1.00$), 30 528 reflections collected at −100 °C, 6617 independent reflections ($R_{int} = 0.0358$), 5277 reflections observed [$I > 2\sigma(I)$], 317 refined parameters, $R_1 = 0.0546$, $wR_2 = 0.1339$ (observed reflections), $R_1 = 0.0707$, $wR_2 = 0.1467$ (all data), max. residual electron density 0.952 and −0.885 e Å^{-3}, Flack $\chi = 0$ after TWIN refinement (initially 0.394(19)).

4.10.4. Crystal/refinement details for ***7***

$C_{31}H_{41}N_3Ni$, $M = 514.38$, red chunk $0.36 \times 0.40 \times 0.56$ mm, orthorhombic, space group $P2(1)2(1)2(1)$, $a = 10.0300(6)$, $b = 11.1256(7)$, $c = 25.2157(16)$ Å, $V = 2813.8(3)$ Å^3, $Z = 4$, $\mu = 0.712$ mm^{-1}, empirical absorption correction ($0.91 \leq T \leq 1.00$), 32 027 reflections collected at −100 °C, 6890 independent reflections ($R_{int} = 0.0293$), 5853 reflections observed [$I > 2\sigma(I)$], 354 refined parameters, $R_1 = 0.0351$, $wR_2 = 0.842$ (observed reflections), $R_1 = 0.0.473$, $wR_2 = 0.0892$ (all data), max. residual electron density 0.428 and −1.114 e Å^{-3}, Flack $\chi = 0$ after TWIN refinement (initially 0.506(12)).

5. Supplementary material

Tables of crystallographic data, atomic coordinates, bond distances and angles, and anisotropic parameters for **4**–**7** as well as chromatograms of branched ethylene oligomers formed by **6** and **7** are available from the author upon request. CIF files have been deposited with the Cambridge Crystallographic Data Centre, CCDC Nos. 199954–199957 for structures **4**–**7**. Copies of this data may be obtained free of charge on application to The Director, CCDC, 12 Union Road, Cambridge CB2 1EZ, UK (fax: +44-1223-336-033; e-mail: deposit@ccdc.cam.ac.uk or www: http://www.cam.ac.uk).

Acknowledgements

We thank Georgetown University for financial support of this work and H.L.W. is grateful to the Georgetown University Research Opportunities Program and the Georgetown Department of Chemistry for summer research fellowships. T.H.W. warmly thanks Professor Richard R. Schrock for his invaluable mentorship.

References

[1] S.D. Ittel, J.K. Johnson, M. Brookhart, Chem. Rev. 100 (2000) 1169.
[2] T.R. Younkin, E.F. Connor, J.I. Henderson, S. Freidrich, R.H. Grubbs, D.A. Bansleben, Science 287 (2000) 460.
[3] W. Keim, A. Behr, B. Limbacker, C. Kruger, Angew. Chem., Int. Ed. Engl. 22 (1983) 503.
[4] W. Keim, R. Appel, S. Gruppe, F. Knoch, Angew. Chem., Int. Ed. Engl. 554 (1987) 1012.
[5] K. Nomura (Ed.), Recent Res. Dev. Pure Appl. Chem., 1998, p. 473.
[6] D. Vogt, in: B. Cornils, W.A. Herrmann (Eds.), Aqueous-Phase Organometallic Chemistry, Wiley-VCH, Weinheim, 1998, p. 541.
[7] W. Keim, Ann. N.Y. Acad. Sci. 415 (1983) 191.
[8] A. Yano, M. Mori, Y. Kondo, JP patent 01014217 to Tosoh Corp., Japan, priority date July 8, 1987.
[9] K.A. Ostoja-Starzewski, J. Witte, Angew. Chem., Int. Ed. Engl. 24 (1985) 599.
[10] K.A. Ostoja-Starzewski, J. Witte, Angew. Chem., Int. Ed. Engl. 26 (1987) 63.
[11] K.A. Ostoja-Starzewski, J. Witte, K.H. Reichert, G. Vasiliou, in: W. Kaminsky, H. Sinn (Eds.), Transition Metals and Organometallics as Catalysts for Olefin Polymerization, Springer, Berlin, 1998, p. 349.
[12] K.A. Ostoja-Starzewski, J. Witte, in: R.P. Quirk (Ed.), Transition Metal Catalyzed Polymerizations—Ziegler–Natta and Metathesis Polymerization, Cambridge University Press, Cambridge, 1988, p. 472.
[13] U. Klabunde, S.D. Ittel, J. Mol. Catal. 41 (1987) 123.
[14] U. Klabunde, R. Mülhaupt, T. Herskovitz, A.H. Janowicz, J. Calabrese, S.D. Ittel, J. Polym. Sci. Part A 25 (1987) 1989.
[15] L.K. Johnson, C.M. Killian, M. Brookhart, J. Am. Chem. Soc. 117 (1995) 6414.
[16] F.C. Rix, M. Brookhart, P.S. White, J. Am. Chem. Soc. 118 (1996) 4746.
[17] C.M. Killian, L.K. Johnson, M. Brookhart, Organometallics 16 (1997) 2005.
[18] S. Mecking, L.K. Johnson, L. Wang, M. Brookhart, J. Am. Chem. Soc. 120 (1998) 888.
[19] D.J. Tempel, M. Brookhart, Organometallics 17 (1998) 2290.
[20] S.A. Svejda, L.K. Johnson, M. Brookhart, J. Am. Chem. Soc. 121 (1999) 10634.
[21] S.A. Svejda, M. Brookhart, Organometallics 18 (1999) 65.
[22] D.J. Tempel, L.K. Johnson, R.L. Huff, P.S. White, M. Brookhart, J. Am. Chem. Soc. 122 (2000) 6686.
[23] J. Ledford, C.S. Shultz, D.P. Gates, P.S. White, J.M. DeSimone, M. Brookhart, Organometallics 20 (2001) 5266.
[24] L.H. Shultz, D.J. Tempel, M. Brookhart, J. Am. Chem. Soc. 123 (2001) 11539.
[25] C.S. Shultz, J.M. DeSimone, M. Brookhart, Organometallics 20 (2001) 16.
[26] L.H. Shultz, M. Brookhart, Organometallics 20 (2001) 3975.
[27] L.K. Johnson, A.M.A. Bennett, S.D. Ittel, L. Wang, A. Parthasarathy, E. Hauptman, R.D. Simpson, J. Feldman, E.B. Coughlin, WO Patent Application 9830609 to DuPont, priority date Jan 4, 1997.
[28] D.A. Banselben, S.K. Friedrich, T.R. Younkin, R.H. Grubbs, C. Wang, R.T. Li, WO Patent Application 9842664 to W.R. Grace & Co, priority date March 24, 1997.
[29] C. Wang, S. Friedrich, T.R. Younkin, R.T. Li, R.H. Grubbs, D.A. Bansleben, M.W. Day, Organometallics 17 (1998) 3149.
[30] F.A. Hicks, M. Brookhart, Organometallics 20 (2001) 3217.
[31] W. Kläui, J. Bongards, G.J. Reiß, Angew. Chem., Int. Ed. Engl. 39 (2000) 3894.

[32] B. Domhöver, W. Kläui, A. Kremer-Aach, R. Bell, D. Mootz, Angew. Chem., Int. Ed. Engl. 37 (1998) 3050.
[33] L.W.M. Lee, W.E. Piers, M.R.J. Elsegood, W. Clegg, M. Parvez, Organometallics 18 (1999) 2947.
[34] W.-K. Kim, M.J. Fevola, L.M. Liable-Sands, A.L. Rheingold, K.H. Theopold, Organometallics 17 (1998) 4541.
[35] P.H.M. Budzelaar, A.B. von Oort, A.G. Orpen, Eur. J. Inorg. Chem. (1998) 1485.
[36] B. Qian, W.J. Scanlon, IV, M.R. Smith, III, D.H. Motry, Organometallics 18 (1999) 1693.
[37] R. Vollmerhaus, M. Rahim, R. Tomaszewski, S. Xin, N.J. Taylor, S. Collins, Organometallics 19 (2000) 2161.
[38] V.C. Gibson, P.J. Maddox, C. Newton, C. Redshaw, G.A. Solan, A.J.P. White, D.J. Williams, Chem. Commun. (1998) 1651.
[39] J. Feldman, S.J. McLain, A. Parthasarathy, W.J. Marshall, J.C. Calabrese, S.D. Arthur, Organometallics 16 (1997) 1514.
[40] P.H.M. Budzelaar, R. de Gelder, A.W. Gal, Organometallics 17 (1998) 4121.
[41] X. Dai, T.H. Warren, Chem. Commun. (2001) 1998.
[42] P.C. Healy, M.R. Bendall, D.M. Doddrell, B.W. Skelton, A.H. White, Aust. J. Chem. 32 (1979) 727.
[43] W.S. Sheldrick, R. Knorr, H. Polzer, Acta Crystallogr., B 35 (1979) 739.
[44] Barnett C. Krüger, J. Organometal. Chem. 42 (1972) 169.
[45] F.A. Cotton, B.A. Frenz, D.L. Hunter, J. Am. Chem. Soc. 96 (1974) 4820.
[46] G.C. Tucci, R.H. Holm, J. Am. Chem. Soc. 117 (1995) 6489.
[47] H.-F. Klein, T. Weimer, Inorg. Chim. Acta 154 (1988) 21.
[48] M. Brookhart, M.L.H. Green, L.-L. Wong, Prog. Inorg. Chem. 36 (1988) 1.
[49] R.R. Schrock, S. Luo, J.J C Lee, N.C. Zanetti, W.M. Davis, J. Am. Chem. Soc. 118 (1996) 3883.
[50] M.E. Thompson, S.M. Baxter, A.R. Bulls, B.J. Burger, M.C. Nolan, B.D. Santarsiero, W.P. Schaefer, J.E. Bercaw, J. Am. Chem. Soc. 109 (1987) 203.
[51] W.W.J. Lukens, M.R. Smith, III, R.A. Andersen, J. Am. Chem. Soc. 118 (1996) 1719.
[52] J.D. Fellmann, R.R. Schrock, D.D. Traficante, Organometallics 1 (1982) 481.
[53] Z. Dawoodi, M.L.H. Green, V.S.B. Mtetwa, K. Prout, J. Chem. Soc., Chem. Commun. (1982) 802.
[54] Z. Dawoodi, M.L.H. Green, V.S.B. Mtetwa, K. Prout, A.J. Shultz, J.M. Williams, T.F. Koetzle, J. Chem. Soc., Dalton Trans. (1986) 1629.
[55] M.D. Fryzuk, S.A. Johnson, S.J. Rettig, J. Am. Chem. Soc. 123 (2001) 1602.
[56] S. Buffagni, L.M. Vallarino, J.V. Quagliano, Inorg. Chem. 3 (1964) 480.
[57] SHELXTL-PC, Version 5.10, Brucker-Analytical X-ray Services, Madison, WI, 1998.
[58] G.M. Sheldrick, SHELX-97, Universität Göttingen, Göttingen, Germany, 1997.
[59] L. Barbour, XSEED, University of Missouri, Columbia, MO, 1999.
[60] G.M. Sheldrick, SADABS, 1996, based on the method described in: R.H. Blessing, Acta Crystallogr., A 51 (1995) 33.